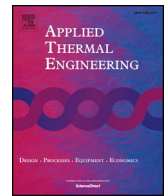




ELSEVIER

Contents lists available at ScienceDirect

Applied Thermal Engineering

journal homepage: www.elsevier.com/locate/apthermeng

Effect of heat exchanger plates geometry on performance of an indirect evaporative cooling system

Stefano De Antonellis^{a,*}, Luca Cignatta^a, Chiara Facchini^a, Paolo Liberati^b

^a Politecnico di Milano, Dipartimento di Energia, Via Lambruschini 4, 20156 Milan, Italy

^b Recuperator S.p.A., Via Valfurva 13, 20027 Rescaldina, MI, Italy



HIGHLIGHTS

- Five systems with different plates geometry are investigated.
- A detailed experimental analysis is carried out.
- Wet bulb effectiveness and pressure drop are evaluated.

ARTICLE INFO

Keywords:

Indirect evaporative cooler
IEC
Geometry
Experimental

ABSTRACT

At present, there is great interest in indirect evaporative coolers (IECs), which can be effectively used to increase energy efficiency of HVAC systems, with particular attention to data center applications. In such devices, performance significantly depends on the formation of an adequate water layer on heat exchanger plates. Therefore, efforts should be made to promote water spreading through an appropriate design of the system.

In this study, an experimental analysis of IECs manufactured with heat exchangers having different geometry is carried out. The scope of the research is to investigate the effect of different plates protrusion and pitch on IEC wet bulb effectiveness and pressure drop. Tests are carried out with counter and parallel air and water flow arrangement.

Results highlight that plates geometry influences both surface wettability and the heat transfer rate. A reticular plates protrusion appears to be a good compromise to enhance system effectiveness. Tests also highlight that the parallel water and secondary air flows arrangement leads to higher wet bulb effectiveness and lower pressure drop compared to the counter flow configuration.

1. Introduction

The energy consumption in the information and communication technology (ICT) sector has increased exponentially over the last years mainly due to the digitization of human activities and technological advances, such as the cloud computing. A key role is played by data centers (DCs) as they are among the largest energy consumers and their energy use is expected to continue increasing by 4% until 2020 [1]. From a global perspective, the data centers sector was estimated to account for 1,1–1,5% of the global electricity consumption in 2011 [2]. In particular, in DCs the fraction of electricity consumption of cooling systems is around 37% [3]: this relevant energy need is related to high thermal loads that should be compensated in server rooms, in order to guarantee the equipment safe operation and to reduce the risk of its premature failure.

Due to the aforementioned reasons, at present there is great interest in reducing energy consumption of data centers. The conventional cooling technology, based on vapour compression cycle, can be replaced or integrated by new efficient technologies based on free cooling. Interest in the application of such systems in ICT facilities is rapidly increasing since the ASHRAE “Thermal Guidelines for Data Processing Environments” have been released [4]. In fact, the recommended air temperature range for data centers has been extended up to 45 °C, making the use of free cooling technologies possible in many working hours of the year. In this context, one of the most promising technologies is the indirect evaporative cooling (IEC) system, which allows to cool the indoor air at constant humidity ratio, hence, without damaging the ICT equipment. A typical IEC unit consists of an air to air heat exchanger, crossed by two airflows, namely the primary and the secondary one. The heat exchanger channels through which the

* Corresponding author.

E-mail address: stefano.deantonellis@polimi.it (S. De Antonellis).

<https://doi.org/10.1016/j.applthermaleng.2020.115200>

Received 26 July 2019; Received in revised form 16 January 2020; Accepted 12 March 2020

Available online 14 March 2020

1359-4311/ © 2020 Elsevier Ltd. All rights reserved.

Nomenclature

<i>A - E</i>	heat exchanger identification letter
<i>cp</i>	specific heat (kJ/kg/K)
<i>D</i>	dry conditions tests
<i>DP</i>	pressure drop tests
<i>h</i>	plates protrusion height (mm)
<i>L_{HE}</i>	gross plates length and width (m)
<i>\dot{m}_a</i>	airflow rate (kg/s)
<i>\dot{m}_w</i>	water flow rate (l/min)
<i>N_{HE}</i>	number of plates (-)
<i>P</i>	pressure (Pa)
<i>pt</i>	plates pitch (mm)
<i>RH</i>	relative humidity (-)
<i>T</i>	dry bulb temperature (°C)
<i>T_{wb}</i>	wet bulb temperature (°C)
<i>u</i>	experimental uncertainty
<i>\dot{V}</i>	volumetric flow rate (m ³ /h)
<i>W</i>	wet conditions tests
<i>x_i</i>	generic measured quantity (-)
<i>X</i>	humidity ratio (kg/kg)
<i>y_i</i>	generic calculated quantity (-)

Greek letters

ρ	density (kg/m ³)
δ	plates thickness (m)
ε_{db}	dry bulb effectiveness (-)
ε_{wb}	wet bulb effectiveness (-)
σ	variance

Superscripts

<i>N</i>	reference condition ($\rho = 1,2 \text{ kg/m}^3$)
----------	---

Subscripts

<i>a</i>	air
<i>min</i>	minimum value (between primary and secondary air-flows)
<i>in</i>	inlet
<i>inst</i>	instrumental
<i>out</i>	outlet
<i>p</i>	primary air stream
<i>s</i>	secondary air stream
<i>w</i>	water
<i>x_i</i>	generic measured quantity
\bar{x}_i	mean of generic measured quantity
<i>y_i</i>	generic calculate quantity

Acronyms

AHU	air handling unit
CF	counter flow
DC	data center
HE	heat exchanger
ICT	information and communication technology
IEC	indirect evaporative cooling / cooler
NTU	number of transfer units
PF	parallel flow

secondary air stream flows are covered with liquid water, which constantly evaporates. Such evaporation process cools down the secondary airflow and the heat exchanger plates, which in turn cool down the primary air stream (whose humidity ratio keeps constant) [5,6]. In data centers applications, the system works in recirculation mode: the primary airflow is extracted from the building and it is supplied back to the indoor environment after being cooled in the indirect evaporative cooling unit. For this reason, indirect evaporative coolers based on conventional M-cycle [7] or in regenerative configuration [8] are not adopted in data centers.

Nowadays there are several ongoing researches on indirect evaporative coolers [9], investigating, through numerical and experimental approaches, the effect on system performance of heat exchanger material and geometry, of airflows layout, of water distribution configuration and of inlet air and water conditions. Interest has also raised in studying new thermodynamic cycles, coupling indirect evaporative cooling systems with conventional technologies.

One of the most critical issues of IEC systems is the water distribution inside the heat exchanger. In fact, the formation of a wide and uniform liquid water film on secondary airflow plates leads to high cooling capacity and reduced apparatus dimensions. For this reason, several studies deal with heat exchanger design and optimization and with airflows and water layout analysis. Regarding the heat exchanger material, it is well known that appropriate hydrophilic coatings can improve surface wettability and IEC performance [10,11]. Materials like zeolite, fibres, carbon and ceramics were applied to IEC heat exchangers as well [12,13].

Heat exchanger features and airflows layout can significantly affect water distribution and IEC system performance. Li et al. [14] discussed the effect of the heat exchanger placement mode (vertical and horizontal) on cooling capacity. Anisimov et al. [15] carried out a numerical study of heat and mass transfer in indirect evaporative air coolers with four air flow arrangements and De Antonellis et al. [16]

experimentally analysed five different airflows configurations of an aluminium alloy heat exchanger. Chengqin et al. [17] and Moshari et al. [18] respectively investigated effects of air to water flow arrangement and indirect - regenerative evaporative cooling systems. Chen et al. [19] carried out a sensitivity analysis in order to optimize the system performance.

Other studies focus on the humidification system: the nozzles setup and the water flow rate supplied to the system influence the IEC effectiveness. In particular, the lower the water flow rate, the poorer the surface wettability and the cooling capacity [20]. In addition, appropriate design and installation of water nozzles can increase system effectiveness, as recently shown by Al-Zubaydi and Hong [21].

In recent years, several plates geometries aimed at improving surface wettability have been investigated: pillow [22], micro-baffled [23], corrugated [24] and diamond shaped [25] plates. It has been experimentally observed that these simple geometries can lead to high wettability. However, none of these studies directly deals with IEC applications.

Therefore, the aim of this work is to investigate how the IEC performance is affected by different heat exchanger plates geometries. The research has been carried out through a detailed experimental analysis of the system, which has been realized in order to meet real industrial needs. In particular, five heat exchangers with different plates geometries have been experimentally analysed adopting the following technical specifications and constraints:

- Heat exchanger plates pitch is equal to 5 mm or 7,35 mm and gross length is equal to 700 mm.
- Plates of heat exchangers are treated with a hydrophilic coating in order to improve surface wettability, according to previous research studies [11].
- Water is supplied in the top of the system to promote a uniform and widespread liquid film [14].

- The water circuit works at low pressure (around 2 bar) and nozzles with wide orifice diameter (around 2 mm) have been used, so as to limit the clogging caused by limestone residuals.

In order to provide useful information to optimize IEC systems, dry and wet bulb effectiveness and pressure drop have been measured for each device in two different flows arrangements.

2. Description of the IEC system and of the test rig

The analysed indirect evaporative cooling system consists of the following main components:

- A cross-flow plate heat exchanger.
- N°2 water nozzles.
- A water pump.
- A water vessel.

According to Fig. 1, the heat exchanger is connected to the air ducts through four plenums. The primary and the secondary air streams flow respectively horizontally and vertically. The water is always supplied in the upper plenum and flows from the top to the bottom of the system. Two different system layouts are evaluated: the counter flow (CF) and the parallel flow (PF) arrangement. In the first case the secondary air stream flows upward (counter current air and water flows arrangement) while in the second one the secondary air stream moves downward (parallel air and water flows arrangement). In both configurations, water is supplied to the airflow through two nozzles, whose nominal flow rate, according to manufacturer data, is equal to 10 l/min at 2 bar. The two nozzles are installed in the top part of the plenum on a manifold that is mounted 50 cm far from the heat exchanger face. The two nozzles are symmetrically installed on the water manifold and the distance between them is equal to 30 cm. The adopted configuration has been chosen to promote the water droplets spreading in the plenum in order to reach a uniform water flux on the heat exchanger face.

The water is collected in a reservoir at the bottom of the system and it is supplied to the nozzles through a constant speed pump. The water flow rate is measured before the manifold and it is manually adjusted through a three way valve installed after the pump. The amount of water evaporated in the IEC system is continuously reintegrated through the aqueduct line. During the tests, water is recirculated from the vessel installed in the bottom of the system. The pump sucks the water from the bottom of the container, at the exit of the IEC system. Therefore, in steady state conditions the inlet and outlet temperature of the water are almost the same.

Pictures of the entire experimental setup, of the top plenum with

water nozzles and of a heat exchanger before its installation in the IEC system are reported in Fig. 2.

According to the scope of the present study, five different heat exchangers have been investigated. The devices are designed and manufactured in order to keep the same external dimensions. In all cases, the plates have squared geometry (gross length equal to 700 mm) and are made of aluminium alloy (thickness equal to 0,14 mm) with a hydrophilic coating, in order to promote the surface wettability [11]. As shown in the scheme of Fig. 3, each plate presents several ribs, spaced by 100 mm, whose height determines the heat exchanger pitch. The airflows move in the channels formed by two consecutive plates and ribs. It is worth specify that adjacent plates are rotated 90° to each other, in order to have a cross flow arrangement. Finally, the plate geometry varies along each channel: seven small semi-spherical dimples (diameter of 12 mm and height of 2 mm), organized in rows perpendicular to the airflow, and a protrusion (if present), with a different shape for each heat exchanger, are periodically impressed.

The five heat exchangers, denoted with a letter (HEs A, B, C, D and E), have different pitch or protrusion geometry, as shown in Fig. 4 and in Table 1. The heat exchanger A is the reference device, with the simplest geometry without protrusions (except for the semi-spherical dimples). The heat exchanger B has the same geometry as A but a reduced pitch (5,00 mm instead of 7,35 mm). Heat exchangers C, D and E have the same pitch of A (7,35 mm) but a different protrusion geometry: in HE C there is a pyramid, in HE D a pyramid with additional deflectors, inserted in order to promote a better water spreading, and, finally, in HE E a lattice. More precisely, in HE D three deflectors are added in the flat area comprised between the main pyramidal protrusion and each rib. The scope of the deflectors is to guide water to the center of the air channel and to promote the water film formation.

Technical specifications of heat exchangers have been chosen in order to evaluate the effect of pitch and protrusion geometry variation on system performance. In the reference device (HE A): *i*) a flat surface is adopted to minimize the influence of protrusions on water distribution; *ii*) the pitch is adopted according to conventional applications in data centers. HE B has been designed to evaluate the effect of the sole variation of plates pitch. Instead, HEs C, D and E have been designed to analyse the influence of the sole variation of the protrusion geometry. More precisely, HE C is a commercial apparatus, HE D consists of a slight modification of HE C and HE E is based on a new lattice geometry aimed to promote water layer formation. In all heat exchangers, the presence of repetitive semi-spherical dimples rows is related to technical constraints of the manufacturing process.

It is worth specifying that due to the presence of the protrusions, HEs C, D and E show high plates stiffness. On the contrary, plates of HEs A and B can be easily bended due to the flat geometry: it is highlighted

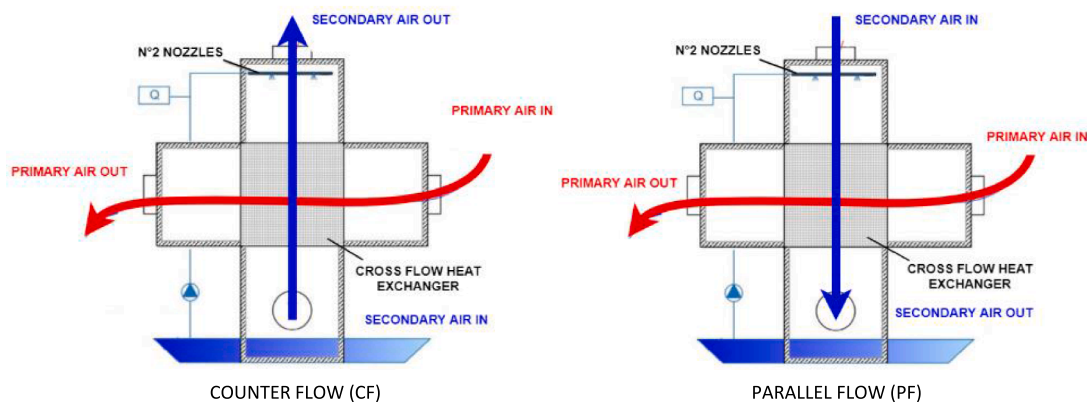


Fig. 1. Scheme of the investigated IEC systems: counter flow (CF) and parallel flow (PF).

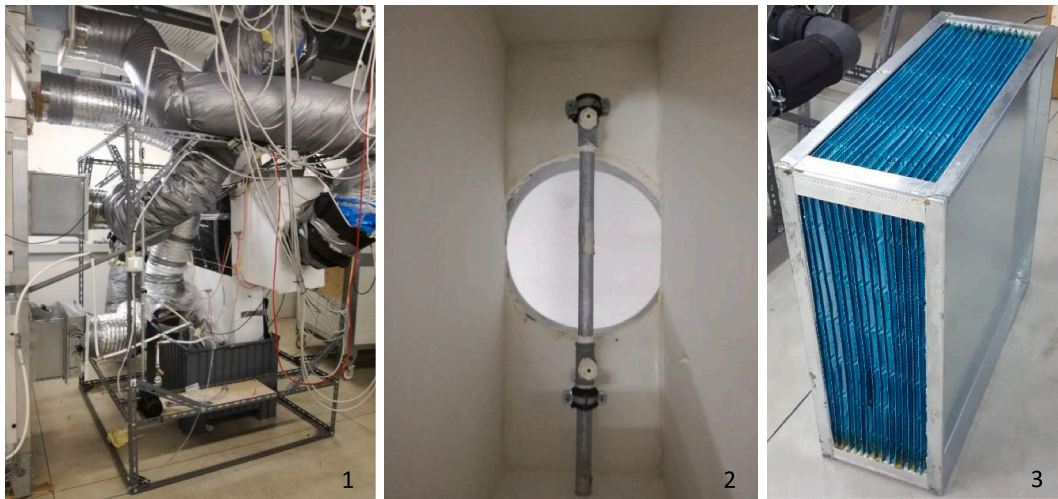


Fig. 2. Experimental setup: (1) View of the system; (2) Detail of the water nozzles installed in the top plenum; (3) View of a heat exchanger.

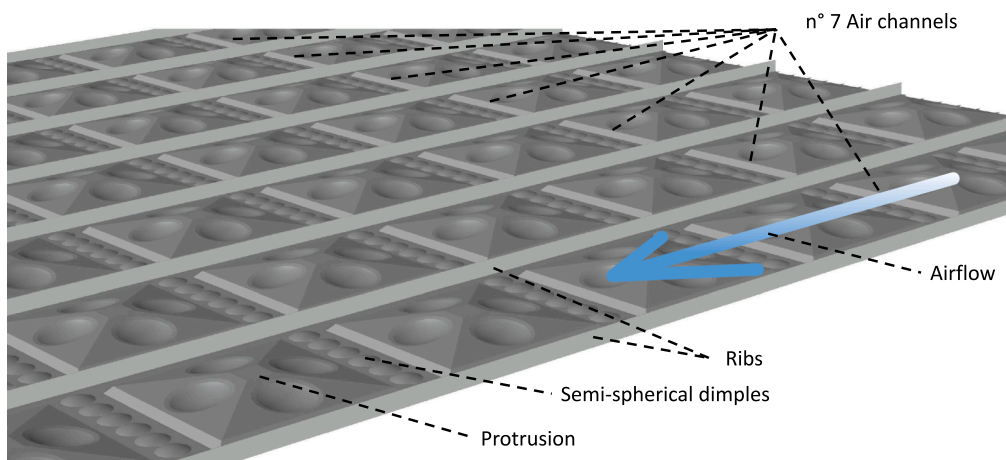


Fig. 3. Generic scheme of heat exchanger plates.

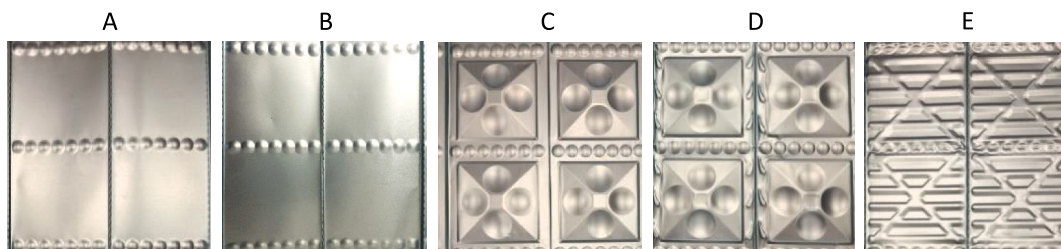


Fig. 4. Pictures of heat exchanger plates (HEs A, B, C, D and E) adopted in the investigated systems.

Table 1
Technical specifications of the five heat exchanger adopted in the IEC system.

		HE A	HE B	HE C	HE D	HE E
Plates gross length	L_{HE} [mm]	700	700	700	700	700
Plates number	N_{HE} [-]	30	46	30	30	30
Plates pitch	pt [mm]	7,35	5,00	7,35	7,35	7,35
Protrusion type	[-]	Flat	Flat	Pyramid A	Pyramid B	Reticular
Protrusion height	h [mm]	0	0	6	6	2
Plates thickness	δ [mm]	0,14	0,14	0,14	0,14	0,14
Gross plates area	A_{tot} [m ²]	13,7	21,5	13,7	13,7	13,7

that this feature could lead to practical limitations in several applications, in particular in case of high pressure difference between the two airflows, because of possible deformation of the channels.

Performance of the investigated system has been evaluated through the following experimental setup: two air handling units (AHUs) treat outdoor airflows through heating and cooling coils and adiabatic humidifiers, in order to reach the desired air conditions. Volumetric flow rates are controlled by variable speed fans and are measured through orifice plates [26] and pressure gauges (accuracy of 0,5% of reading ± 1 Pa). A detailed description of the test rig has been reported in a previous work [16]. The connections between the plenums and the AHUs are realized through insulated flexible ducts. Coupled temperature (PT 100, accuracy of $\pm 0,2$ °C at 20 °C) and relative humidity (capacitive sensor, accuracy of $\pm 1\%$ between 0 and 90% at 20 °C) probes and differential pressure gauges (accuracy of 1,5% of reading ± 1 Pa) have been installed at the inlet and outlet of each airflow. Finally, water stream rate is measured through a vortex sensor (accuracy of $\pm 2\%$). It is worth specifying that, due to space limitations, pressure probes have been placed in the inlet and outlet plenums, close to the heat exchanger faces. Therefore, it is expected that pressure drop measurements could be affected by the not uniform velocity field. For this reason, obtained results should be preferably used to compare different heat exchangers or operating conditions and not for a precise evaluation of pressure drop.

3. Experimental methodology and test conditions

In this study, performance of the indirect evaporative cooler has been measured through the following indexes: the dry bulb effectiveness ε_{db} , the wet bulb effectiveness ε_{wb} and the secondary air pressure drop ΔP_s . The parameters are defined as:

$$\varepsilon_{db} = \frac{\dot{m}_p c_{p,p} (T_{p,in} - T_{p,out})}{(\dot{m}_a c_{p,a})_{min} (T_{p,in} - T_{s,in})} \quad (1)$$

$$\varepsilon_{wb} = \frac{T_{p,in} - T_{p,out}}{T_{p,in} - T_{wb,s,in}} \quad (2)$$

$$\Delta P_s = P_{s,in} - P_{s,out} \quad (3)$$

Tests are carried out in steady state conditions and temperature, relative humidity and pressure difference are recorded every second. According to international standards [27,28], the uncertainty of directly measured and of calculated quantities is respectively determined in the following way:

$$u_{x_i} = \pm \sqrt{u_{x_i,inst}^2 + (t_{95} \sigma_{x_i})^2} \quad (4)$$

$$u_{y_i} = \sqrt{\sum_i \left(\frac{\partial y_i}{\partial x_i} u_{x_i,inst} \right)^2 + t_{95}^2 \sum_i \left(\frac{\partial y_i}{\partial x_i} \sigma_{x_i} \right)^2} \quad (5)$$

Further details about uncertainty calculations are reported in a previous work of the authors [20].

Several tests of the indirect evaporative cooler, aimed at evaluating the performance of the different heat exchanger plates pitch (HEs A and B) and protrusion geometry (HEs A, C, D and E) in representative data

center operating conditions, have been carried out. As summarized in Table 2, three different types of experimental tests have been conducted:

- Tests in dry conditions to evaluate ε_{db} (denoted with *D*).
- Tests in wet conditions to evaluate ε_{wb} (denoted with *W*).
- Tests in dry and wet conditions to evaluate secondary air pressure drop (denoted with *DP*).

The experimental analysis has been carried out both in counter flow (CF) and parallel flow (PF) arrangement (Fig. 1).

With reference to values of Table 2, inlet dry bulb air temperature and humidity ratio were set with a tolerance respectively of ± 1 °C and ± 0.5 g/kg. Airflow rates are always referred to a reference density ($\rho = 1,2$ kg/m³). In addition, results of dry and wet tests have been considered acceptable when the difference between energy exchanged by primary and secondary airflow was within 5%. Finally, it is highlighted that when the airflow rate assumed the minimum (900 m³/h) or maximum (1800 m³/h) value, the corresponding air face velocity (before HE entrance) was respectively around 1,6 m/s and 3,2 m/s. Inlet air temperature and humidity ratio have been selected in order to reproduce representative conditions of IECs operating in data centers [11,16,20]. Instead, airflow rates are adopted to have typical and adequate air velocity along heat exchanger plates.

The experimental campaign has been carried out through the following main steps:

1. The configuration with HE A (no protrusion and $pt = 7,35$ mm) and counter flow (CF) arrangement has been selected as reference case. In particular, the CF layout was selected because representative of practical applications [29–31].
2. Performances of the reference system in dry and wet operating conditions were evaluated and obtained results compared.
3. Tests of IEC with HE A in PF arrangement were carried out and results were compared with ones of the reference case, in order to evaluate the effect of flows configuration.
4. Tests of IEC with HE B in CF layout have been performed and the effect of plates pitch was therefore analysed.
5. Tests of IEC with HEs C, D and E in CF layout were carried out to investigate the effect of protrusion geometry.

Experimental results are described and analysed in Section 4, following the aforementioned approach.

4. Experimental results

4.1. Test in dry conditions

In this section, performances in dry conditions of the five heat exchangers are measured and compared. The scope of this investigation is to collect data about conventional heat exchange capacity of the devices and, at the same time, to have reference information to understand the behaviour of the devices in the further tests in wet conditions.

In Fig. 5, the dry bulb effectiveness of the five heat exchangers is

Table 2
Adopted conditions of dry, wet and pressure drop tests.

	$T_{p,in}$ [°C]	$T_{s,in}$ [°C]	$X_{p,in}$ [g/kg]	$X_{s,in}$ [g/kg]	$\dot{V}_{p,in}^N$ [m ³ /h]	$\dot{V}_{s,in}^N$ [m ³ /h]	\dot{m}_w [l/min]
<i>D</i>	35	20	5	5	1000;1100;1200	1000;1100;1200	–
<i>W1</i>	35	25	5	10	1800	900	3;4;5;7;9
<i>W2</i>	35	25	5	10	1800	1200	3;4;5;7;9
<i>W3</i>	35	30	5	13,5	1800	900	3;4;5;7;9
<i>DP0</i>	20	20	5	5	–	900;1200;1500;1800	–
<i>DP5</i>	20	20	5	5	–	900;1200;1500;1800	5
<i>DP9</i>	20	20	5	5	–	900;1200;1500;1800	9

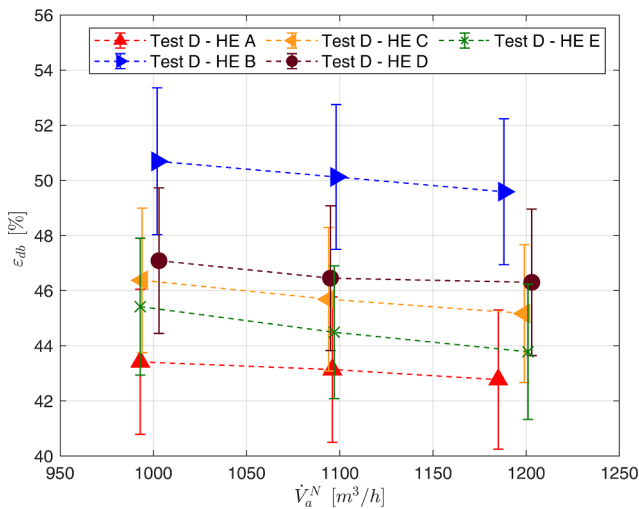


Fig. 5. Dry bulb effectiveness of the investigated five IEC systems.

reported at balanced airflows. HE A shows the lowest ϵ_{db} because of the high plates pitch ($pt = 7,35$ mm), which leads to low total heat exchanger area at constant overall dimensions, and the absence of plates protrusions, which leads to a low heat transfer rate. HE B presents the highest effectiveness due to the low plates pitch ($pt = 5$ mm): in fact, as reported in Table 1, in this device A_{tot} is around 50% higher than those of HEs A, C, D and E. In particular, ϵ_{db} of HE B is around 8% higher than that of HE A. Dry bulb effectiveness of HEs C, D and E, which are all designed with the same plates pitch ($pt = 7,35$ mm) but with different protrusions geometry, is always within the extreme values measured for HE A and B. The presence of the protrusions increases the heat transfer rate and ϵ_{db} of HEs C, D and E is from 1% to 4% higher than that of HE A. Although measured dry bulb effectiveness of HE D is the highest among devices with high plates pitch ($pt = 7,35$ mm), the difference is quite limited and within the experimental uncertainty. In addition, quite obviously the dry bulb effectiveness of the five heat exchangers always decreases with the airflow rate, due to the reduction in NTU.

Finally, it is highlighted that also the presence of the semi spherical dimples, which are impressed in all channels of the five devices, contributes to increase the heat transfer rate. Therefore, the effectiveness of HEs A and B is higher (more than 10%) than the one of heat exchangers with the same plates pitch and length but with perfectly flat surface (dry bulb effectiveness estimated through heat transfer correlations available in literature [32,33] and the ϵ_{db} - NTU approach [34]).

4.2. Test in wet conditions

4.2.1. Effect of operating conditions

Although the scope of this study is the analysis of IEC systems based on heat exchangers with different features, a concise investigation of the effect of airflows conditions on performance is presented. The effect of working conditions on system effectiveness has been deeply discussed in previous research papers [11,16,20] for similar IECs.

In Fig. 6 the wet bulb effectiveness of HE A is reported as a function of the water flow rate for different operating conditions W1, W2 and W3, as illustrated in Table 2. The following considerations are pointed out:

- A raise in the water flow rate up to 6 l/min leads to an increase in the wet bulb effectiveness. However, a further raise in $\dot{m}_{w,in}$ (6–9 l/min) doesn't increase the cooling capacity and ϵ_{wb} . Such trend can be explained by considering that the additional water supplied to the systems does not evaporate and tends to flow along the same preferential paths, without any significant increase in the wet fraction of the channel area. For instance, in case W1, the humidity ratio

variation of the secondary airflow ($X_{s,out} - X_{s,in}$), which is a direct indication of the evaporated water, is 6,1 g/kg at $\dot{m}_{w,in}$ equal to 3 l/min and reaches 6,4 g/kg when $\dot{m}_{w,in}$ is increased to 7–9 l/min.

- The air inlet conditions influence the wet bulb effectiveness: at a given water flow rate, ϵ_{wb} of test W3 is higher than one obtained in test W1 in spite of the reduction of the primary air temperature difference. For instance, at $\dot{m}_{w,in}$ equal to 9 l/min, the process air temperature variation in case W3 is 5,8 °C while in case W1 is 7,1 °C. This trend can be explained considering that the secondary air inlet wet bulb temperature of test W3 ($T_{wb,s,in} \sim 22$ °C) is higher than one of test W1 ($T_{wb,s,in} \sim 18$ °C), leading to an increase in ϵ_{wb} due to the reduction of denominator of Eq. (2).
- The secondary airflow rate influences the IEC wet bulb effectiveness: the higher \dot{V}_s^N , the higher ϵ_{wb} . Comparing tests W1 and W2, which are carried out with the same inlet air conditions but with different secondary airflow rate (\dot{V}_s^N respectively equal to 900 m³/h and 1200 m³/h) it is possible to state that the heat exchange increases with \dot{V}_s^N . This effect is mainly related to the secondary air inlet temperature $T_{s,in}$, which is lower than the primary air inlet temperature $T_{p,in}$. In this condition, the heat exchanged between the two flows would increase also in dry conditions. Anyway, it should be clarified that if $T_{s,in} > T_{p,in}$, an increase in \dot{V}_s^N doesn't necessarily lead to an increase in ϵ_{wb} , as already discussed in literature [11]. Finally, considering that the same $T_{p,in}$ and $T_{wb,s,in}$ were adopted in tests W1 and W2, an increase in wet bulb effectiveness is directly related to an increase in the primary air temperature variation (for example, at $\dot{m}_{w,in}$ equal to 9 l/min, in cases W1 and W2 the difference $T_{p,in} - T_{p,out}$ is respectively equal to 7,1 °C and 7,6 °C).

For a detailed discussion about the effect of the independent variation of $T_{s,in}$, $X_{s,in}$, $T_{wb,s,in}$ and \dot{V}_s^N , which is not the scope of this work, it is suggested to refer to previous experimental researches [11,16,20]. It is highlighted that measured performance trends of this work are in agreement with results of such studies, even if ϵ_{wb} values are not directly comparable because of the different configuration (plates geometry, pitch and coating; air and water flow arrangement) and operating conditions of the IEC systems.

4.2.2. Effect of secondary airflow arrangement

In this section, the effect of water flow arrangement, namely counter flow (CF) and parallel flow (PF), on wet bulb effectiveness and on

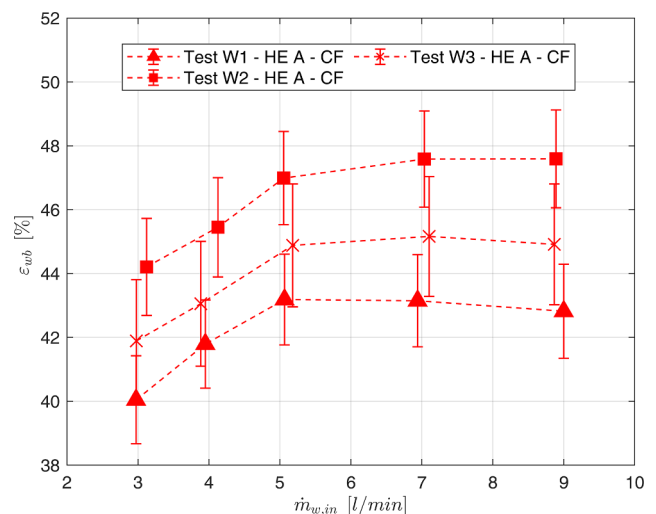


Fig. 6. Effect of water flow rate and operating conditions (W1: $T_{s,in} = 25$ °C, $X_{s,in} = 10$ g/kg, $\dot{V}_s^N = 900$ m³/h; W2: $T_{s,in} = 25$ °C, $X_{s,in} = 10$ g/kg, $\dot{V}_s^N = 1200$ m³/h; W3: $T_{s,in} = 30$ °C, $X_{s,in} = 13,5$ g/kg, $\dot{V}_s^N = 900$ m³/h); on wet bulb effectiveness (HE A in CF arrangement).

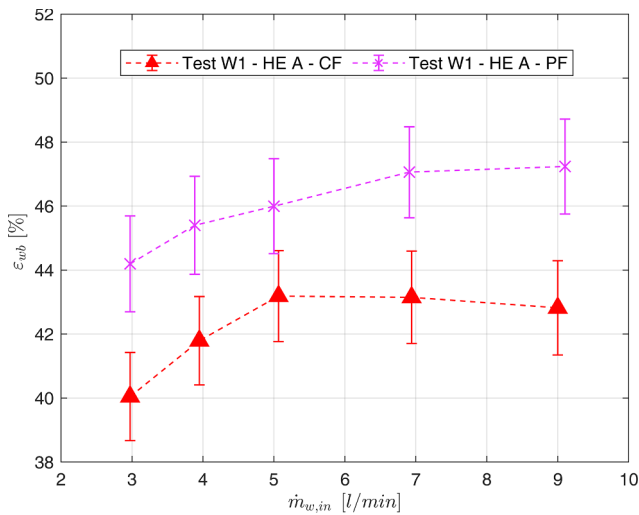


Fig. 7. Effect of water flow rate and airflow arrangement (CF: Counter Flow; PF: Parallel Flow) on wet bulb effectiveness (HE A in test condition W1).

pressure drop is discussed. The analysis is carried out for IEC system with HE A.

In Fig. 7, wet bulb effectiveness against water flow rate is plotted for CF and PF arrangement (test W1). At a given $\dot{m}_{w,in}$, ϵ_{wb} obtained with parallel water and secondary air flow is significantly higher (around 4%) than the one obtained in CF configuration. Such experimental data seem to be in contrast with numerical results available in literature [17,35], which suggest a counter flow configuration to increase system performance (at a given wet surface fraction). This difference can be explained considering that in the actual system, in PF arrangement, the water distribution on heat exchanger plates is promoted by the airflow and, therefore, the average wettability factor is different from CF configuration. In addition, in PF arrangement water droplets are not dragged outside the system but they are forced to pass in the heat exchanger channels with, consequently, an increase in plates wet surface fraction.

Finally, according to explanation reported in Section 4.2.1, in both cases only a raise in the water flow rate up to 6 l/min leads to an increase in the wet bulb effectiveness.

In Fig. 8, pressure drop versus secondary airflow rate is shown in dry condition (DP0) and with water flow rate equal to 5 l/min (DP5) and to 9 l/min (DP9) for CF and PF arrangement. The following considerations are highlighted:

- Quite obviously, the higher the secondary airflow rate, the higher the pressure drop (due to the increase in the air velocity along the channels).
- In dry conditions, pressure drop is clearly not dependent on flows arrangement. Pressure drops in DP0 conditions of CF and PF configurations are overlapped.
- At a given secondary airflow rate, pressure drop in PF arrangement is almost independent on water flow rate. This can be explained by the fact that the water film distribution is promoted by the air, as the two streams flow in the same direction, and thin water layer doesn't reduce significantly the air channel section.
- At a given secondary airflow rate, pressure drop in CF arrangement strongly depends on water flow rate. This phenomenon can be explained considering that water and air move in opposite direction, leading to an instability of the water flow front that creates a barrier to the air stream, with consequent high pressure drop in wet mode.
- In CF configuration, pressure drops in tests DP5 and DP9 are similar. This phenomenon is probably related to the similar wavy water flows, which lead to a comparable pressure drop.

4.2.3. Effect of plates pitch

In order to evaluate how heat exchanger pitch influences the performance of the IEC system, wet bulb effectiveness and pressure drop of HEs A and B are compared. According to data reported in Table 1, the two devices differ for the plates pitch: 7,35 mm for HE A and 5 mm for HE B.

Fig. 9 shows the wet bulb effectiveness of the two systems against water flow rate in test W1. In these operating conditions, ϵ_{wb} of HE B is always higher (around 10%) than the one of HE A: such significant difference is mainly due to the higher dry bulb effectiveness, which is related to the larger heat transfer area.

It is highlighted that HE B has been tested also in PF configuration. In this case, wet bulb effectiveness is around 2–3% higher than one in CF arrangement in the entire 3–9 l/min water flowrate range. Results are in agreement with ones of HE A discussed in Section 4.2.2.

In Fig. 10, pressure drops of HEs A and B are shown in dry and wet test conditions. In dry conditions (test DP0), at a given airflow rate, the highest ΔP_s is measured in case of HE B, due to the higher friction factor. When water is supplied to the system (tests DP5 and DP9), a significant increase in pressure drop is observed for both devices, according to the considerations already reported in Section 4.2.2.

4.2.4. Effect of plates geometry

In this section, a comparison of performance of HEs A, C, D and E is discussed. Main characteristics and geometric data of heat exchangers are reported in Table 1. Since the plates protrusion geometry (flat for HE A, pyramid for HE C, pyramid with additional deflectors for HE D, lattice for HE E) is the only difference among the four devices, it is possible to investigate how it influences the performance in wet operating conditions. As shown in Fig. 11, for a given $\dot{m}_{w,in}$, the wet bulb effectiveness is similar in the four case studies, with a difference between best and worst apparatus of 2%. It is highlighted that:

- Although HE A shows the lowest dry bulb effectiveness (Fig. 5), performance in wet conditions is close to ones of HEs C and E. The nearly flat plate channel geometry doesn't promote heat transfer but it enhances the formation of a uniform water film and, therefore, it promotes water evaporation due to the higher fraction of wet surface.
- In wet conditions HE D performs worse than HE C even if the dry bulb effectiveness is higher. Therefore, deflectors introduced along the protrusion do not effectively promote water film formation.
- HE E seems to be a good compromise among the different investigated protrusion geometries. The reticular pattern contributes

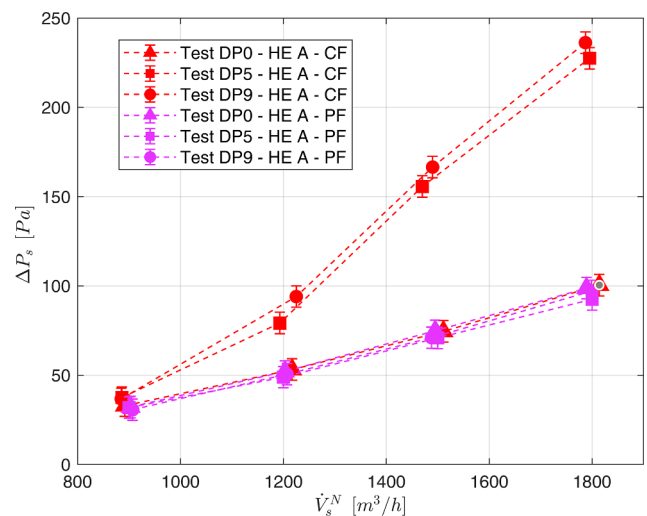


Fig. 8. Effect of water and air flow rate and airflow arrangement (CF: Counter Flow; PF: Parallel Flow) on pressure drop (HE A).

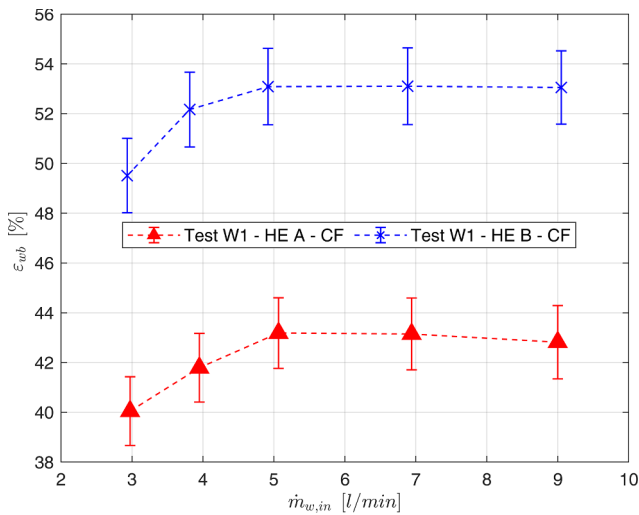


Fig. 9. Effect of water flow rate and plates pitch (HE A: 7,35 mm; HE B: 5,00 mm) on wet bulb effectiveness (test W1, CF arrangement).

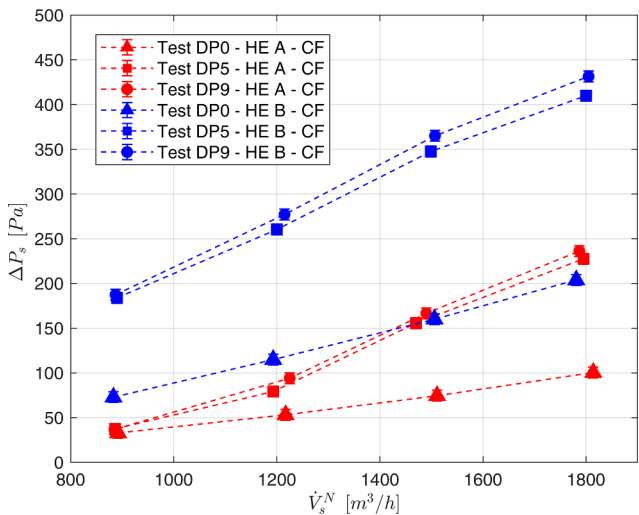


Fig. 10. Effect of water and airflow rate and plates pitch (HE A: 7,35 mm; HE B: 5,00 mm) on pressure drop (CF arrangement).

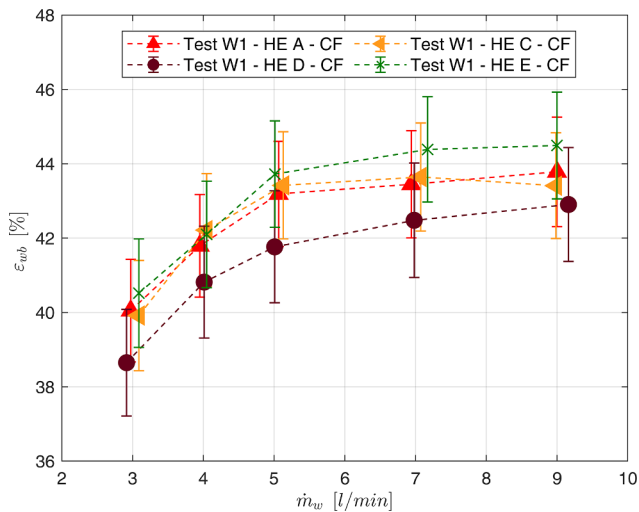


Fig. 11. Effect of water flow rate and plates geometry (HE A: Flat; HE C: Pyramid A; HE D: Pyramid B; HE E: Reticular) on wet bulb effectiveness (test W1, CF arrangement).

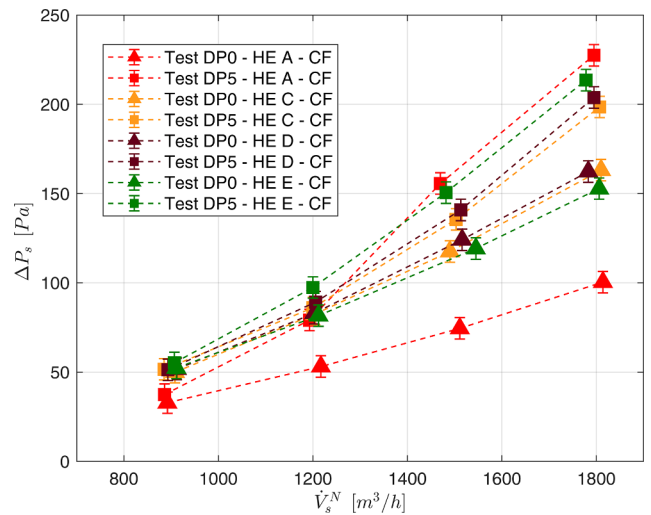


Fig. 12. Effect of water and air flow rate and plates geometry (HE A: Flat; HE C: Pyramid A; HE D: Pyramid B; HE E: Reticular) on pressure drop in dry and wet conditions (CF arrangement).

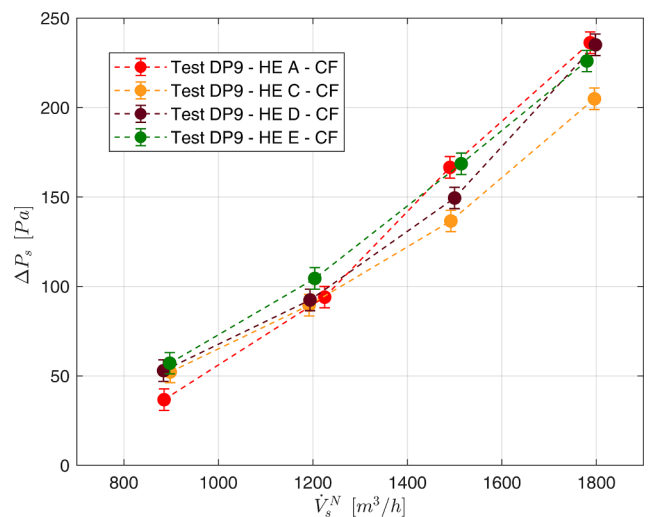


Fig. 13. Effect of water and air flow rate and plates geometry (HE A: Flat; HE C: Pyramid A; HE D: Pyramid B; HE E: Reticular) on pressure drop in wet conditions (CF arrangement).

at the same time to increase the heat transfer and to promote the water film formation.

Further tests of HES C, D and E in downward secondary airflow arrangement (PF) have been carried out (condition W1). Results highlight that also in this configuration ϵ_{wb} is around 4–6% higher than in CF layout in the entire water flowrate range, as discussed in section 4.2.2 for HE A. Finally, a few tests in CF arrangement and in condition W2 (high secondary airflow rate) have been carried out: at $\dot{m}_{w,in}$ equal to 9 l/min, the wet bulb effectiveness of HE D and E is respectively 47,6% and 49,1%. Therefore, the increase in ϵ_{wb} is comparable with one of HE A discussed in Section 4.2.1.

In Figs. 12 and 13, pressure drops in dry and wet conditions of the four heat exchangers are shown:

- In tests DP0 (no water supplied to the system), HE A shows the lowest pressure drop due to the limited variation of the velocity field along the channels. Instead, HE C and HE D, which have a similar pyramidal protrusion, present the highest pressure drop mainly because of the highest protrusion height.

- In wet conditions (*DP5* and *DP9*), HE *C* shows the smallest pressure drop. This is probably due to the fact that the pyramids tend to break the wave front created by the two-phase counter flow, diverting the water to the lateral zone of the channels. This phenomenon allows to reduce the obstructed channels cross section and, therefore, to slightly limit pressure drop. HE *A* shows the highest pressure drop due to the flat geometry that does not guide water to the lateral area of the channel, leading to flow instabilities reported in Section 4.2.2.
- The presence of deflectors along channels does not influence significantly the pressure drop, being measurements of HE *D* similar to those of HE *C*.

5. Conclusions

In this research, five indirect evaporative cooling systems have been investigated. Each system is characterized by a heat exchanger with different plates geometry. Experimental tests have been carried out in several dry and wet conditions and in different flows arrangement. System performance is evaluated in typical operating conditions of data centers. Hereinafter, main obtained results are summarized:

- Flat plates geometry promotes the surface wettability but does not guarantee high heat transfer rates and an adequate system stiffness.
- Complex plates protrusions tend to enhance the heat transfer but, at the same time, to limit the formation of a wide and uniform water layer.
- The reticular protrusion appears to be a good compromise between overall heat transfer, wettability and stiffness of plates.
- Tests results highlight that the parallel water and air flows arrangement lead to higher wet bulb effectiveness and lower pressure drop compared to the counter flow configuration.
- In all configurations, the optimal water flow rate is around 5–9 l/min. No significant differences among the five IECs are observed.
- In the parallel flow configuration, pressure drop is almost independent on water flow rate. On the contrary, in counter flow arrangement the presence of the water significantly increases the pressure drop.
- In the investigated conditions, HE *E* provides higher dry bulb effectiveness (up to 2%) and wet bulb effectiveness (up to 1%) compared to HE *A*. Pressure drop is lower in wet conditions (up to –30%) and higher in dry conditions (up to 50%). In addition, plates stiffness is significantly increased.

Declaration of Competing Interest

The authors declare that they have no known competing financial interests or personal relationships that could have appeared to influence the work reported in this paper.

Acknowledgments

The authors acknowledge Recuperator S.p.A. personnel, in particular Mr Leone, Mr Martello and Mr Bawa for the technical and economic support and Mrs Imperatore and Mr Picarella for the help to manufacture the tested IEC systems.

Funding for this work from Regione Lombardia (Italy) under agreement n° E47H18000490007 are acknowledged (Innodriver 2017 - Misura A).

References

- [1] A. Shehabi, S. Smith, D. Sartor, R. Brown, M. Herrlin, J. Koomey, E. Masanet, N. Horner, I. Azevedo, W. Lintner, United states data center energy usage report, 2016.
- [2] H. Rong, H. Zhang, S. Xiao, C. Li, C. Hu, Optimizing energy consumption for data centers, *Renew. Sustain. Energy Rev.* 58 (2016) 674–691.
- [3] M. Antal, T. Cioara, I. Anghel, C. Pop, I. Salomie, Transforming data centers in active thermal energy players in nearby neighborhoods, *Sustainability* 10 (4) (2018) 939.
- [4] ASHRAE, *Thermal Guidelines for Data Processing Environments*, 4th ed. 2015.
- [5] D. Pandelidis, A. Cichoń, A. Pacak, S. Anisimov, P. Drag, Counter-flow indirect evaporative cooler for heat recovery in the temperate climate, *Energy* 165 (2018) 877–894.
- [6] G. Zhu, T.T. Chow, C.K. Lee, Performance analysis of counter-flow regenerative heat and mass exchanger for indirect evaporative cooling based on data-driven model, *Energy Build.* 155 (2017) 503–512.
- [7] H.S. Dizaji, E.J. Hu, L. Chen, A comprehensive review of the Maisotsenko-cycle based air conditioning systems, *Energy* 156 (2018) 725–749.
- [8] X. Cui, M.R. Islam, B. Mohan, K.J. Chua, Developing a performance correlation for counter-flow regenerative indirect evaporative heat exchangers with experimental validation, *Appl. Therm. Eng.* 108 (2016) 774–784.
- [9] Z. Duan, C. Zhan, X. Zhang, M. Mustafa, X. Zhao, B. Alimohammadisagvand, A. Hasan, Indirect evaporative cooling: Past, present and future potentials, *Renew. Sustain. Energy Rev.* 16 (9) (2012) 6823–6850.
- [10] J. Lee, D.Y. Lee, Experimental study of a counter flow regenerative evaporative cooler with finned channels, *Int. J. Heat Mass Transf.* 65 (2013) 173–179.
- [11] M. Guilizzoni, S. Milani, P. Liberati, S. De Antonellis, Effect of plates coating on performance of an indirect evaporative cooling system, *Int. J. Refrig.* (2019).
- [12] X. Zhao, S. Liu, S.B. Riffat, Comparative study of heat and mass exchanging materials for indirect evaporative cooling systems, *Build. Environ.* 43 (11) (2008) 1902–1911.
- [13] F. Wang, T. Sun, X. Huang, Y. Chen, H. Yang, Experimental research on a novel porous ceramic tube type indirect evaporative cooler, *Appl. Therm. Eng.* 125 (2017) 1191–1199.
- [14] W.Y. Li, Y.C. Li, L.Y. Zeng, J. Lu, Comparative study of vertical and horizontal indirect evaporative cooling heat recovery exchangers, *Int. J. Heat Mass Transf.* 124 (2018) 1245–1261.
- [15] S. Anisimov, D. Pandelidis, Theoretical study of the basic cycles for indirect evaporative air cooling, *Int. J. Heat Mass Transf.* 84 (2015) 974–989.
- [16] S. De Antonellis, C.M. Joppolo, P. Liberati, Performance measurement of a cross-flow indirect evaporative cooler: Effect of water nozzles and airflows arrangement, *Energy Build.* 184 (2019) 114–121.
- [17] R. Chengqin, Y. Hongxing, An analytical model for the heat and mass transfer processes in indirect evaporative cooling with parallel/counter flow configurations, *Int. J. Heat Mass Transf.* 49 (3–4) (2006) 617–627.
- [18] S. Moshari, G. Heidarnejad, A. Fathipour, Numerical investigation of wet-bulb effectiveness and water consumption in one-and two-stage indirect evaporative coolers, *Energy Convers. Manage.* 108 (2016) 309–321.
- [19] Y. Chen, H. Yang, Y. Luo, Parameter sensitivity analysis and configuration optimization of indirect evaporative cooler (IEC) considering condensation, *Appl. Energy* 194 (2017) 440–453.
- [20] S. De Antonellis, C.M. Joppolo, P. Liberati, S. Milani, L. Molinaroli, Experimental analysis of a cross flow indirect evaporative cooling system, *Energy Build.* 121 (2016) 130–138.
- [21] A.Y.T. Al-Zubaydi, G. Hong, Experimental study of a novel water-spraying configuration in indirect evaporative cooling, *Appl. Therm. Eng.* (2019).
- [22] K. Siebeneck, W. Popov, T. Stefanak, S. Scholl, Pillow plate heat exchangers-investigation of flow characteristics and wetting behavior at single-flow conditions, *Chemie Ingenieur Technik* 87 (3) (2015) 235–243.
- [23] H. Ishikawa, S. Ookawara, S. Yoshikawa, A study of wavy falling film flow on micro-baffled plate, *Chem. Eng. Sci.* 149 (2016) 104–116.
- [24] A. Gonda, P. Lancereau, P. Banelier, L. Luo, Y. Fan, S. Benezech, Water falling film evaporation on a corrugated plate, *Int. J. Therm. Sci.* 81 (2014) 29–37.
- [25] D. Patil, R. Kumar, F. Xiao, Wetting enhancement of polypropylene plate for falling film tower application, *Chem. Eng. Process. Process Intensif.* 108 (2016) 1–9.
- [26] DIN EN ISO 5167-2 Standards, Measurement of fluid flow by means of pressure differential devices inserted in circular cross-section conduits running full—Part 2: Orifice plates (ISO 5167-2:2003).
- [27] ISO IEC Guide 98-3, Uncertainty of Measurement—Part 3: Guide to Expression of Uncertainty in Measurement, International Organization for Standardization, ISO IEC Guide 98-3, Geneva Switzerland, 2008.
- [28] Evaluation of measurement data – Guide to the expression of uncertainty in measurement JCGM 100:2008 (GUM 1995 with minor corrections).
- [29] M. Rampazzo, M. Lionello, A. Beghi, E. Sisti, L. Cecchinato, A static moving boundary modelling approach for simulation of indirect evaporative free cooling systems, *Appl. Energy* 250 (2019) 1719–1728.
- [30] P.E. Keith Dunnivant, Data center heat rejection, *ASHRAE* 3 (2011) 44–54.
- [31] S. Delfani, J. Esmaeelian, H. Pasdarshahri, M. Karami, Energy saving potential of an indirect evaporative cooler as a pre-cooling unit for mechanical cooling systems in Iran, *Energy Build.* 42 (11) (2010) 2169–2176.
- [32] V. Gnielinski, On heat transfer in tubes, *Int. J. Heat Mass Transf.* 63 (2013) 134–140.
- [33] V. Gnielinski, Corrigendum to “On heat transfer in tubes” [International Journal of Heat and Mass Transfer 63 (2013) 134–140], *Int. J. Heat Mass Transf.* 100 (81) (2015) 638.
- [34] ESDU 98005, Design and performance evaluation of heat exchangers: the effectiveness and NTU method, Engineering and Sciences Data Unit 98005 with Amendment A, London ESDU International plc., 1998, pp. 122–129.
- [35] K.J. Chua, J. Xu, X. Cui, K.G. Ng, M.R. Islam, Numerical heat and mass transfer analysis of a cross-flow indirect evaporative cooler with plates and flat tubes, *Heat Mass Transf.* 52 (2016) 1765–1777.